

Molecular conductors with differently oriented conducting layers, $(\text{EDT-TTF})_3\text{Hg}_2\text{Br}_6$ and $(\text{TMBEDT-TTF})_5\text{Hg}(\text{SCN})_{4-x}\text{I}_x$

E. I. Zhilyaeva,^{a*} V. N. Semkin,^b E. I. Yudanov,^a R. M. Vlasova,^b S. A. Torunova,^a A. M. Flakina,^a G. A. Mousdis,^c K. V. Van,^d A. Graja,^e A. Lapinski,^e R. B. Lyubovskii,^a and R. N. Lyubovskaya^a

^aInstitute of Problems of Chemical Physics, Russian Academy of Sciences,
1 prosp. Akad. Semenova, 142432 Chernogolovka, Moscow Region, Russian Federation.
Fax: + 7 (496) 515 5420. E-mail: zhilya@icp.ac.ru

^bA. F. Ioffe Physico-Technical Institute, Russian Academy of Sciences,
26 ul. Politekhnikeskaya, 194021 St. Petersburg, Russian Federation

^cTheoretical and Physical Chemistry Institute, NHRF, 11635 Athens, Greece

^dInstitute of Experimental Mineralogy, Russian Academy of Sciences,
4 ul. Institutskaya, 142432 Chernogolovka, Moscow Region, Russian Federation

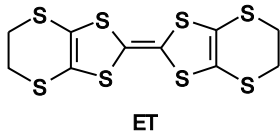
^eInstitute of Molecular Physics, Polish Academy of Sciences,
60179 Poznan, Poland

New conducting radical cation salts $(\text{EDT-TTF})_3\text{Hg}_2\text{Br}_6$, $(\text{TMET})_5\text{Hg}(\text{SCN})_{4-x}\text{I}_x$ ($x \approx 0.35$), and $(\text{EDT-TTF})_3\text{Hg}(\text{SCN})_{3.05}(\text{PhCl})_{0.5}$ were synthesized. Their conductivities, ESR and polarized reflectance spectra were studied. It was shown that the organic conductors with differently oriented conducting layers $(\text{EDT-TTF})_3\text{Hg}_2\text{Br}_6$ and $(\text{TMET})_5\text{Hg}(\text{SCN})_{4-x}\text{I}_x$ ($x \approx 0.35$) are characterized by the quasi-one-dimensional character of electron motion. The conductivity along and across conducting layers has a semiconductive character. It was established by ESR and polarized reflectance spectroscopy that the properties of such conductors are a superposition of the properties of individual conducting layers.

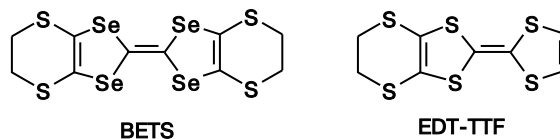
Key words: molecular conductors based on radical cation salts, electrical conductivity, polarized reflectance spectra, ESR spectra.

Molecular conductors based on radical cation salts are widely investigated in recent decades. On cooling, many of these compounds exhibit metallic properties and undergo phase transitions into the superconducting or dielectric state.^{1,2} Their structures and properties strongly depend on counterions that determine the character of the radical cation salts. The mercury-containing anions with the halogen, thiocyanate, and mixed-type ligands with diverse compositions and structures are used as counterions. A whole class of low-dimensional molecular conductors based on the radical cation salts with the mercury-containing metal complexes as anions has arisen.^{3,4}

The radical cation salts with the thiocyanatomercurate anions with the composition $(\text{ET})_x\text{MHg}(\text{SCN})_4$ (ET is bis(ethylenedithio)tetrathiafulvalene, M is a monovalent cation), depending on the nature of the cation M, are characterized by a wide range of electroconducting properties, from semiconducting to superconducting ones (see Ref. 4 and references cited therein). The crystals of molecular conductors with the mixed halogenothiocyanoanions



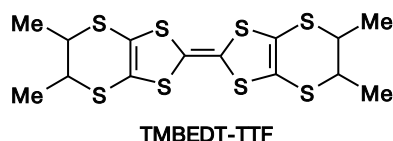
$(\text{ET})_2\text{Hg}(\text{SCN})_{3-n}\text{X}_n$ ($\text{X} = \text{F}, \text{Cl}, \text{Br}, \text{I}$) undergo the phase transitions of the type metal–insulator upon lowering of temperature.³ Among the radical cation salts with the halogenomercurate anions, there are superconductors $(\text{ET})_4\text{Hg}_{2.89}\text{Br}_8$ (see Refs 3, 5), $(\text{ET})_4\text{Hg}_{2.78}\text{Cl}_8$ (see Ref. 3), $(\text{BETS})_4\text{Hg}_{2.84}\text{Br}_8$ (see Ref. 6), and $(\text{EDT-TTF})_4(\text{Hg}_3\text{I}_8)_{1-x}$ (see Ref. 7) and conductors remaining the metallic state in a wide temperature range,^{8,9} as well as conductors manifesting the transition metal–insulator^{3,10–12} (BETS is bis(ethylenedithio)tetrathiafulvalene, EDT-TTF is ethylenedithiotetrathiafulvalene).



In general, layered conductors based on radical cation salts are built of conducting layers with identical orientations of stacks of the radical cations. However, among the radical cation salts with the stacked structure of the conducting layer, several compounds are known, for which the orientations of stacks in the adjacent conducting

layers are different: these are the superconductors β'' -(ET)₄(H₃O)M(C₂O₄)₃(PhCN)¹³, the semiconductor (TMTSF)₃[Y(NO₃)₅]₂(PhCl)¹⁴ (TMTSF is tetramethyltetraselenafulvalene, Y is ittrium), the organic metals (BETS)₄MBr₄(PhX)^{15,16}, and the conductors with the composition α - β'' -(ET)₄NH₄M(C₂O₄)₃(Solv)¹⁷ (Solv is PhNMeCHO, PhCH₂CN, PhCOMe) and β' - θ -(ET)₂-[C(SO₂CF₃)₃] characterizing by the transition metal—insulator at 150–180 K.¹⁸ In the latter case, the stacks from the adjacent layers differ in both the orientation and structure.

The preparation and investigation of new electroconducting radical cation salts with differently oriented conducting layers that are characterized by reduced dimensionality of the electron system are important for discovery of new physical properties and more in-depth study of the nature of electronic phenomena in organic conductors. In addition, the layered crystals with different structures and/or different orientations of conducting layers can serve as nanocomposites consisting of the layers with somewhat different properties. It is important to establish whether the properties of such a system is a superposition of properties of individual layers or a new ground state arises.⁴ In the present work, we considered the relationship between the properties and structures of the layered organic conductors (EDT-TTF)₃Hg₂Br₆, (TMBEDT-TTF)₅-Hg(SCN)_{4-x}I_x, and (EDT-TTF)₃Hg(SCN)₃I_{0.5}(PhCl)_{0.5}.



Results and Discussion

Based on the electron-donating molecules of ethylenedithiotetrathiafulvalene³ and bis(dimethylethylenedithio)tetrathiafulvalene (TMBEDT-TTF), we synthesized new radical cation salts (EDT-TTF)₃Hg₂Br₆ (**1**) and (TMBEDT-TTF)₅Hg(SCN)_{4-x}I_x ($x \approx 0.35$) (**2**) with different stacking directions in the adjacent conducting layers and studied their electroconductivities, ESR and polarized reflectance spectra. For comparison, compound (EDT-TTF)₃Hg(SCN)₃I_{0.5}(PhCl)_{0.5} (**3**) with identical stack orientations in the conducting layers was synthesized. In the presently known salts EDT-TTF and TMBEDT-TTF, the adjacent conducting layers are built of unidirectional stacks.^{19,20}

Salts **1**–**3** were prepared by electrochemical oxidation of the corresponding tetrathiafulvalene (EDT-TTF or TMBEDT-TTF) in the presence of tetrabutylammoniummercury(II) salts {Bu₄NHgBr₃ + HgBr₂} or [Bu₄N]CsHg(SCN)_{3.5}I_{0.5}. In the presence of the tribromomercurate(II) anion, EDT-TTF forms a salt with

another stoichiometric composition, viz., (EDT-TTF)₂-HgBr₃, along with salt **1**. Upon increase in the HgBr₂: Bu₄NHgBr₃ ratio in the supporting electrolyte from 5 : 1 to 50 : 1, the composition of electrocrystallization products was not changed. Electrochemical oxidation of EDT-TTF and TMBEDT-TTF in the presence of [Bu₄N]CsHg(SCN)_{3.5}I_{0.5} affords the salts only with the mixed iodothiocyanaatomercurate(II) anions. All compounds were obtained as single crystals with the β -type packing of conducting layers, i.e., they are composed of the stacks of one type.²¹ According to the data from X-ray diffraction,²² the angle between the stack orientations of the adjacent conducting layers is 79–80° for crystals of **1** and 73–76° for crystals of **2**. In the single crystal of **3**, the stack orientations for all conducting layers are identical.²² The availability of single crystals allowed us to study the longitudinal and cross conductivities, the ESR and polarized reflectance spectra.

The conductivities of the crystals of **2** in the shape of elongated hexagonal plates with dimensions of 2×1.2×0.1 mm were studied for two directions ($\sigma_{\parallel 1}$ and $\sigma_{\parallel 2}$) in the plane of the plate (hereinafter referred to as the conducting plane) and perpendicular (σ_{\perp}) to this plane. For the crystals of **1** and **3** having smaller dimensions, $\sigma_{\parallel 1}$ and σ_{\perp} were studied. Table 1 shows the room-temperature conductivities of compounds under study, as well as the ratio of conductivities along and across the conducting layers, which characterizes crystal anisotropy. As a comparison, the data²⁰ on the conductivity anisotropy of compound (TMBEDT-TTF)₃(ClO₄)₂ are given. It follows from the data of Table 1 that the conductivity in the plane of the plate for the crystal of **2** with differently oriented conducting layers is almost isotropic ($\sigma_{\parallel 1} : \sigma_{\parallel 2} = 3$), while the conductivity in the layer for the crystals of (TMBEDT-TTF)₃(ClO₄)₂ with identical stack orientations in the conducting layers²⁰ is significantly anisotropic ($\sigma_{\parallel 1} : \sigma_{\parallel 2} = 300$).

Upon reduction of the temperature, the conductivity along layers in the crystals of **1**, **2**, and **3** has a semicon-

Table 1. The room-temperature conductivity and anisotropy of conductivity of the crystals of **1**–**3** and (TMBEDT-TTF)₃(ClO₄)₂*

Crystal	$\sigma_{\parallel 1}$	$\sigma_{\parallel 2}$	σ_{\perp}	$\sigma_{\parallel 1} : \sigma_{\parallel 2} : \sigma_{\perp}$
	/S cm ⁻¹			
1	6	—	$2 \cdot 10^{-2}$	300 : 1
2	2	0.6	$2 \cdot 10^{-3}$	1000 : 300 : 1
3	80	—	$2 \cdot 10^{-2}$	4000 : 1
(TMBEDT-TTF) ₃ (ClO ₄) ₂	—	—	—	1000 : 3 : 1 ²⁰

* $\sigma_{\parallel 1}$ and $\sigma_{\parallel 2}$ are conductivities of crystals for two orientations in the \parallel^2 plane parallel to the crystal plane; σ_{\perp} is a conductivity in the direction perpendicular to the crystal plane; $\sigma_{\parallel 1} : \sigma_{\parallel 2} : \sigma_{\perp}$ is anisotropy of conductivity.

ductive character with the activation energies (E_a) of about 0.09, 0.05, and 0.01 eV, respectively. The electron state of salts **2** and **3** in the temperature range of ~230–200 K and 170–160 K changes into the semiconductive state with higher activation energies of ~0.24 and ~0.025 eV, respectively. Upon lowering of the temperature from 200 to 70 K, the activation energy in salt **1** decreases *ca.* ninefold and, at the temperature less than 70 K, E_a becomes constant and is ~0.01 eV.

Thus, all compounds under study exhibit the semiconductive character of temperature dependence of conductivity with variable activation energies. The study of the conductivity of salt **2** in the conducting plane suggests that the character of the electron system is close to isotropic in two orientations.

ESR spectroscopy allows one to obtain information on the crystal packing and electronic structure of organic conductors based on radical cation salts, as well as on structural phase transformations occurring upon the temperature change. The analysis of experimental data reported in Ref. 1 showed that the ESR linewidth (ΔH_{pp}) of the radical cation salts based on ET is a characteristic parameter, which is related to the structural packing of radical cations in the layer. This allows one to suggest the packing motif of radical cations in the conducting layer according to the ESR linewidth and to use the parameter ΔH_{pp} for identification of various crystalline phases of the radical cation salts based on ET.¹

Depending on the sample orientation, the room-temperature ESR spectra of all compounds under study had the Lorentz- or Dyson-type shape. If the microwave electric field was parallel to the conducting plane of the crystal, the Dyson line appears due to the formation of the skin layer and nonuniform distribution of electric and magnetic fields throughout the sample bulk.^{23,24} At room temperature, the ratio of the low-field portion of the Dyson line to the high-field one (A/B) is 1.5, 1.86, and 1.3 for salts **1**, **2**, and **3**, respectively. The Dyson-type line shape evidences high conductivity in radical cation salts.

According to the X-ray diffraction data,²² all salts under study have the β -type packing of the cationic layer. However, depending on the crystal orientation in the resonator cavity, the ESR linewidths (ΔH_{pp}) of the compounds under study are 6–7.5 G for **1** and 7–8.5 G for **2** and **3**, which is *ca.* twofold smaller than in the quasi-two-dimensional ET salts with the β -type packing. Such values of ΔH_{pp} are typical of the quasi-one-dimensional salts based on tetrathiafulvalene.²³ As a comparison, in the quasi-two-dimensional organic metal with the composition β -(EDT-TTF)₄(Hg₃I₈)_{1-x} (see Ref. 7), the linewidth is ~20–22 G, which is typical of the β -type salts. Thus, the narrow ESR lines of the studied compounds together with the sufficiently high conductivity suggest the quasi-one-dimensional character of electron motion.

We studied the dependences of the g -factor and ΔH_{pp} of compounds **1** and **2** (Fig. 1) on crystal orientation in the magnetic field. The character of such dependences is sinusoidal and, for the g -factor, is determined by the change in the g -tensor of crystal, which can be expressed in the molecular system of coordinates by the equation

$$g^2 = \sum g_{ij}^2 (\cos i \cdot \cos j),$$

where g_{ij} are the anisotropic components of the g -tensor and $\cos i$ and $\cos j$ are the directional cosines relative to the molecular axes i and j . The linewidths of the organic conductors and the g -factor are interrelated by the Elliot formula and change in parallel upon rotation of a crystal in the magnetic field. However, for the crystals of **1** and **2** whose feature is different stack orientation in the adjacent conducting layers, an unusual character of the angular dependence of ΔH_{pp} at such sample orientation when the rotation axis of the crystal coincident with the microwave field direction H_1 is perpendicular to the conducting layer and the constant magnetic field H_0 is parallel to the conducting plane (Fig. 1, *c*, *d*) was found. The maxima of ΔH_{pp} appear upon rotation of the crystal by ~90°, while the g -factor changes upon rotation by 180°. Probably, this is associated with overlapping of the signals for the adjacent differently oriented conducting layers, the Elliot formula being not valid for the crystals of **1** and **2**. In the quasi-two-dimensional organic metal β'' -(ET)₄(NH₄)Cr(C₂O₄)₃(DMF) having also different stack orientations in the adjacent layers (the angle of ~70°), the iteration of maxima typical of radical cation salts was observed after rotation by 180° with ΔH_{pp} changing little (within 27–30 G).²⁴ However, in the structure of β'' -(ET)₄(NH₄)Cr(C₂O₄)₃(DMF), the ET⁺· planes from the adjacent layers are almost parallel whereas, in **1** and **2**, the planes of radical cations from the adjacent layers are almost perpendicular.

The temperature dependences of ΔH_{pp} and spin susceptibilities (χ) of compounds **1**, **2**, and **3** in the range of 140–293 K are shown in Fig. 2. In all compounds, ΔH_{pp} decreases with reduction of the temperature, however, for **1**, ΔH_{pp} begins to increase at the temperature below 160 K. The spin susceptibility (χ) of this compound remains almost constant upon reduction of the temperature to 160 K and then begins to increase, which probably evidences the appearance of the localized electrons in the conducting radical cation layer. In contrast to salt **1**, salt **2** shows the temperature behavior of spin susceptibility typical of the Heisenberg homogeneous antiferromagnetic chain¹ and described by the Bonner–Fischer model. In the case of compound **3** with identical stack orientations in the layers, a qualitative change in the temperature dependence of the parameter χ occurs at 210–220 K, which indicates the transition from the activation susceptibility to the Curie-type dependence typical of the localized spins.

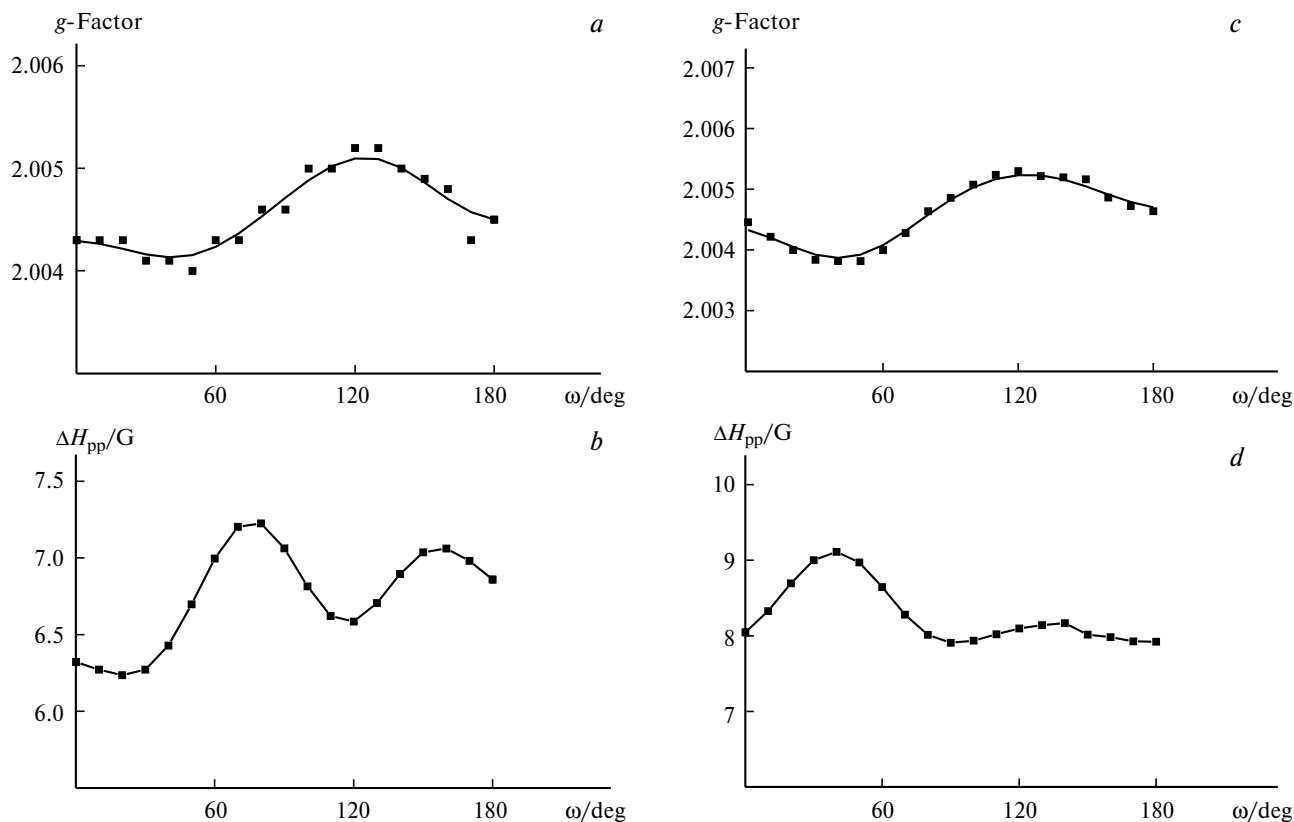


Fig. 1. The dependence of the g-factor (*a*, *c*) and ESR linewidth (ΔH_{pp}) (*b*, *d*) of the crystals of **1** (*a*, *b*) and **2** (*c*, *d*) on the rotation angle of the crystal in the magnetic field upon horizontal setting of the crystal.

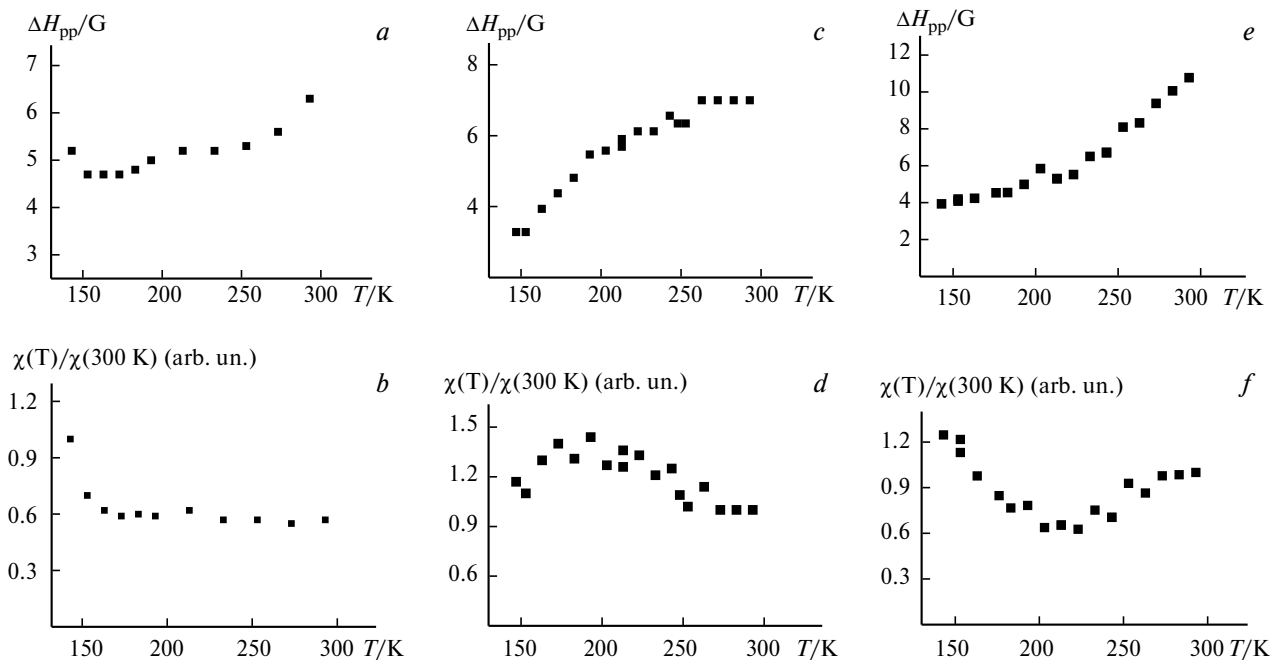


Fig. 2. The temperature dependence of the ESR linewidth (*a*, *c*, *e*) and relative spin susceptibility (*b*, *d*, *f*) of the crystals of **1** (*a*, *b*), **2** (*c*, *d*), and **3** (*e*, *f*).

Thus, the results of the investigation of the ESR spectra suggest different character of the electronic spin interactions in the conducting layers of these compounds and the structural reorganizations that occur in compounds **1** and **3** upon lowering of the temperature and result in the states with the localized spins.

For the electroconducting organic radical ion salts, the relevant information on the state of electronic system can be retrieved from the polarized reflectance spectra. In these spectra, high reflectance in the low-frequency region with the plasma edge of reflectance typical of metals and the effects associated with the interaction of intramolecular vibrations with the conductivity electrons are observed.^{25–27} We studied the polarized reflectance spectra of the crystals of salts **1**, **2**, and **3** in the frequency range of 700–6500 cm^{-1} for two orientations in the crystal plane parallel to the conducting layers.

Figure 3 shows the polarized reflectance spectra of the crystal of **1** at 300 and 8 K. The reflectance spectra were measured in the polarizations wherein the electric vector of the optical wave E is parallel (E_{\parallel}) and perpendicular (E_{\perp}) to the main diagonal of the rhombic plate. This means that E is parallel to the stack orientations in the adjacent conducting layers (the angle between the stacks is 79–80°). At 300 K, in both incident light polarizations, high electronic reflectance (up to 0.7) with the pronounced plasma

edge near 5000–5500 cm^{-1} and an intense vibrational structure of the spectrum in the region of 1000–1500 cm^{-1} caused by electron-vibrational interaction (EVI) are observed. In the optical conductivity spectra, the broad electronic band with the maximum at 1300 cm^{-1} (0.16 eV) caused by the intraband electron transition is complicated by the deep notch at 1350 cm^{-1} associated with EVI. The intraband transition corresponds to the charge-transfer process $(\text{EDT-TTF})^0 + (\text{EDT-TTF})^+ \rightarrow (\text{EDT-TTF})^+ + (\text{EDT-TTF})^0$. The position of electronic bands, the absence of anisotropy, and sufficiently high optical conductivity (more than 700 S cm^{-1} at 700 cm^{-1}) suggest the isotropic character of the electronic system of this compound in two orientations, which is caused by overlapping of the optical responses of the quasi-one-dimensional stacks in the adjacent layers, since, according to the X-ray diffraction data, the stack orientations in the adjacent conducting layers are virtually orthogonal. At 8 K, the reflectance of crystal **1** in the region of 700–1500 cm^{-1} is significantly lower ($R \approx 0.5$) and there was a change in the character and intensity of the vibrational structure in both polarizations. The optical conductivity spectra at 8 K have the pattern typical of semiconductors. The observable shifts of electronic maxima from 1300 cm^{-1} (0.16 eV) to 2430 cm^{-1} (0.3 eV) for the orientation along acute angle bisectrix of the rhombic plate and to 1790 cm^{-1} (0.22 eV)

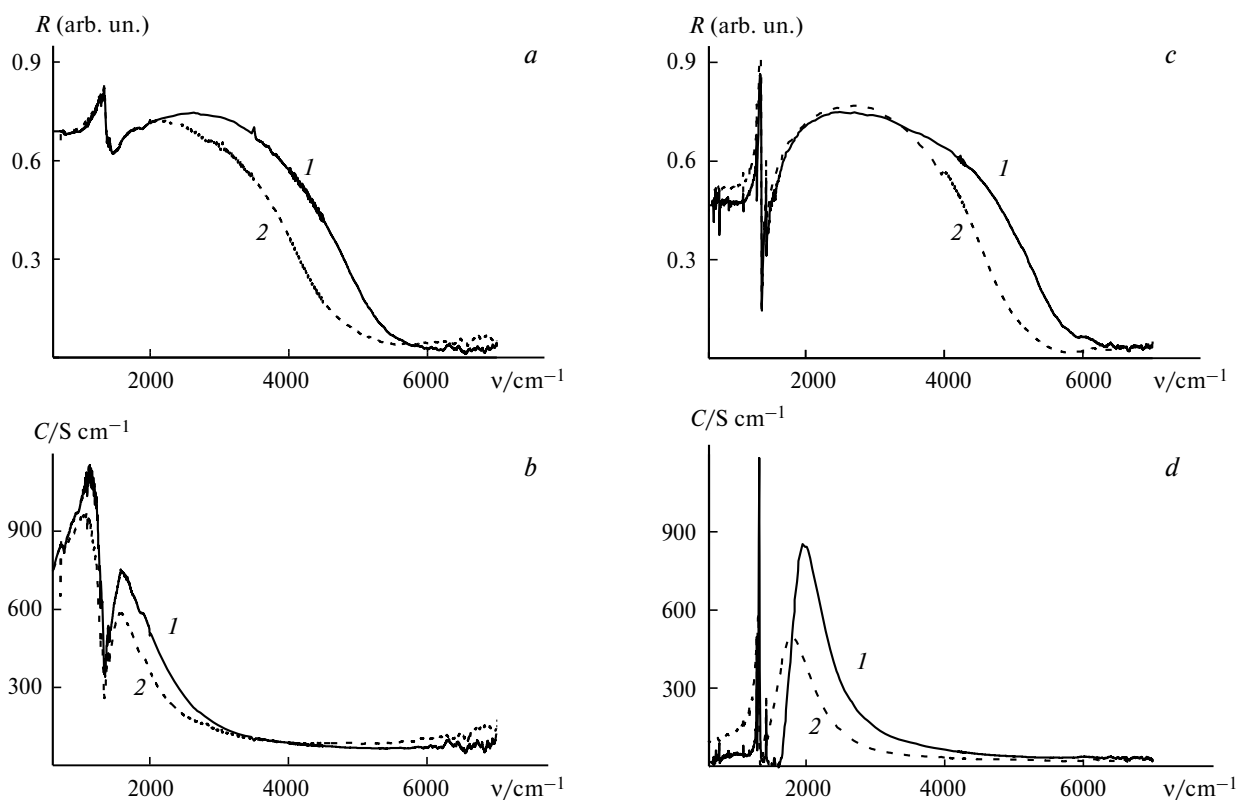


Fig. 3. The reflectance (*a*, *c*) and optical conductivity (*b*, *d*) spectra of the crystals of **1** in the polarizations perpendicular (*1*) and parallel (*2*) to the long crystal axis at 300 (*a*, *b*) and 8 K (*c*, *d*).

for the orthogonal orientation evidence the increase in the intraband electron transition energy, which may be due to possible structural reorganizations within the radical cation clusters. The term "cluster" (see Ref. 28) means the packing of n radical cations into " n -mers", the overlap integrals of the wave functions outside and inside " n -mer" being different. The ESR spectral data indicate probable structural changes in the radical cation layers. The vibrational features in the optical conductivity at 8 K appear as narrow intense bands on the frequencies corresponding to the vibrations of the EDT-TTF molecule (intense lines on the frequencies of 1324, 1424, 1289 cm^{-1} and less intense lines on the frequencies of 1224, 1186, 1094, 882, 749, 695, and 665 cm^{-1}). The different positions of the electronic maxima for two polarizations suggest the differences in the electronic structure of the adjacent conducting layers in the crystal of **1** at 8 K.

Figure 4 shows the polarized reflectance spectra of the crystal of **3** at 300 and 8 K measured in two orientations: parallel (E_{\parallel}) and perpendicular (E_{\perp}) to the long axis of the platelike crystal. It is seen from Fig. 4 that the reflectance spectra have the patterns typical of the quasi-one-dimensional conducting crystals: the reflectance in the polarization E_{\parallel} is about $R \approx 0.4$ in the wide spectral region from 700 to 4000 cm^{-1} and the fuzzy plasma edge having the minimum in the region of 7500–8000 cm^{-1} is observed

upon increase in the frequency. The strong vibrational feature positioned on the frequency of 1350 cm^{-1} is caused by the electron-vibrational interaction of the quasi-one-dimensional electronic system with the intramolecular vibrations of the fragments EDT-TTF in the stacks. The reflectance in the polarization E_{\perp} is weak ($R \approx 0.18$ –0.2) and slightly changes with the change in the light frequency. The optical conductivity spectrum calculated from the Kramers–Kronig relations has the pattern typical of semi-conductive compounds in the polarization E_{\parallel} : the electronic band with the maximum at 3000 cm^{-1} (0.37 eV) and the half width of 2950 cm^{-1} , the low-frequency wing of which has the peak at 1319 cm^{-1} . Upon reduction of the temperature, the maximum of the electronic band for the orientation E_{\parallel} in the optical conductivity spectrum is shifted to 1800 cm^{-1} (0.22 eV) and noticeably shrunk to 670 cm^{-1} . These changes in the optical conductivity spectra seems to be associated with the increase in the number of radical cations comprising the clusters. The vibrational feature at 8 K has the shape of a "hook" with the maximum at 1305 cm^{-1} and satellites at 1290 and 1430 cm^{-1} . In the polarization E_{\perp} , the reflectance and optical conductivity spectra change slightly upon reduction of the temperature. Thus, the analysis of the optical properties shows that, at 300 and 8 K, the crystals of **3** are characterized by the quasi-one-dimensional electronic structure of conducting layers.

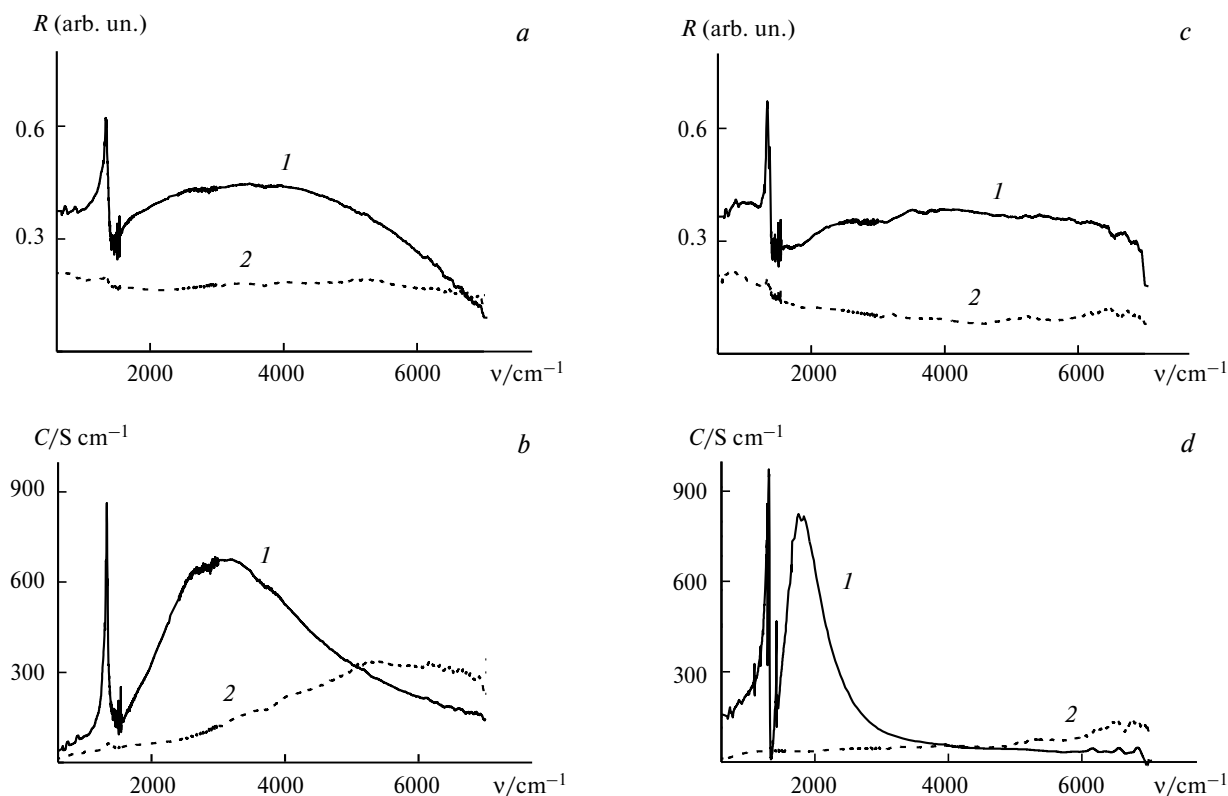


Fig. 4. The reflectance (a, c) and optical conductivity (b, d) spectra of the crystals of **3** in the polarizations parallel (1) and perpendicular (2) to the long crystal axis at 300 (a, b) and 8 K (c, d).

The polarized reflectance spectra of the crystal of **2** at 300 and 5 K are shown in Fig. 5. The reflectance spectra are measured in the polarizations at where the electric vector of the light wave E is parallel (E_{\parallel}) and perpendicular (E_{\perp}) to the long axis of the platelike crystal, which approximately coincides with the stack orientations of TMBEDT-TTF in the adjacent layers. At 300 K, the spectra of salt **2** display the electronic reflectance ($R \approx 0.5$ for E_{\parallel} and $R \approx 0.4$ for E_{\perp} at low frequencies) with the intense vibrational structure in the region of 1500 cm^{-1} , which is smaller as compared with compound **1**. In contrast to **1**, the crystal of **2** shows weak anisotropy at 300 K (which agrees well with the conductivity anisotropy of this salt): the spectra for two main orientations E_{\parallel} and E_{\perp} in the crystal plane parallel to the conducting layers somewhat differs in the intensity, the positions of both reflectance maxima and minima in the spectra being close. The plasma edge at 4000 cm^{-1} is well defined for the orientation E_{\parallel} in the crystal, whereas the reflectance edge for another orientation, viz., E_{\perp} , is poorly defined. In the low-frequency region, the growth and relatively high reflectance remain in both polarizations. The optical conductivity spectra at 300 K are characterized by a weak anisotropy in the conducting plane (the maximum optical conductivity along E_{\parallel} reaches the value of 300 S cm^{-1} compared to 200 S cm^{-1} in the orientation E_{\perp}). The vibration-

al feature is characterized by the deep notch at 1500 cm^{-1} (0.186 eV) being approximately in the maximum of intra-band electron transition. In our opinion, the reason for the weak anisotropy of the reflectance spectra of compound **2** having the one-dimensional stacks of the TMBEDT-TTF radical cations in the layer is overlapping of the optical response of the alternating quasi-one-dimensional layers with the orthogonal stack orientations as in the case of the crystal of **1**. At 5 K, the reflectance spectra of salt **2** display decrease in the reflectance in the low-frequency region (to $R \approx 0.25$ in both polarizations) and the spectra become more isotropic for the orientations E_{\parallel} and E_{\perp} . The optical conductivity spectra calculated for the reflectance spectra at $T = 5\text{ K}$ acquire the form typical of dielectric: the gap forms in the low-frequency region of the spectrum of electronic states, the electronic maximum is shifted to 2200 cm^{-1} (0.27 eV) at 5 K compared to 1500 cm^{-1} (0.186 eV) at 300 K, and the electronic-vibration feature acquires the form of the peak on the flank of electronic line at 1410 cm^{-1} with the satellites on the frequencies of 1435 and 1442 cm^{-1} . The above-mentioned changes in the optical conductivity spectrum of the crystal of **2** upon reduction of temperature correlate well with the changes in the corresponding spectra of the crystal of **1** and are caused by structural reorganization in the clusters of the corresponding cations. At 5 K, the reflectance and optical

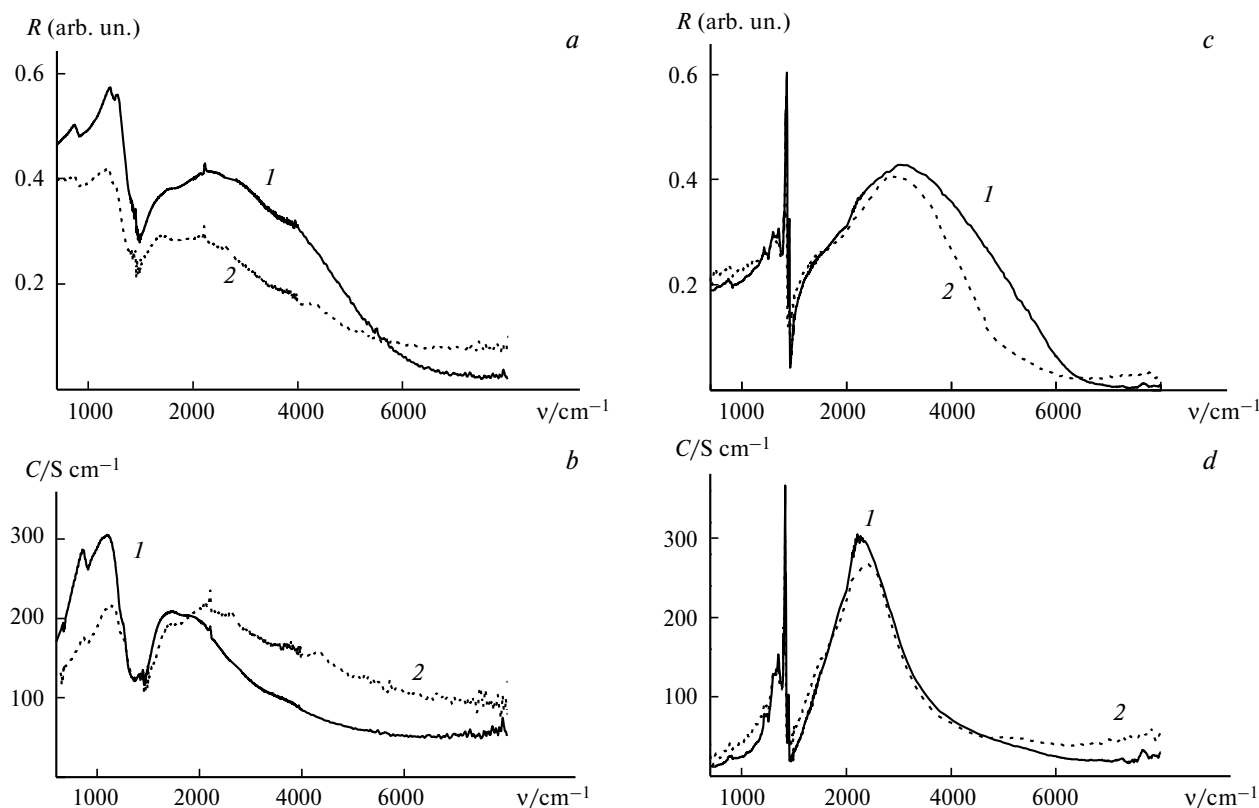


Fig. 5. The reflectance (a, c) and optical conductivity (b, d) spectra of the crystals of **2** in the polarizations parallel (I) and perpendicular (2) to the long crystal axis at 300 (a, b) and 5 K (c, d).

conductivity spectra become isotropic for two orientations in the plane of conducting layers.

Thus, in the present work, we synthesized new organic conductors based on the electron-donating compounds TMBEDT-TTF and EDT-TTF with the composition $(\text{EDT-TTF})_3\text{Hg}_2\text{Br}_6$, $(\text{TMBEDT-TTF})_5\text{Hg}(\text{SCN})_{4-x}\text{I}_x$ ($x \approx 0.35$), and $(\text{EDT-TTF})_3\text{Hg}(\text{SCN})_3\text{I}_{0.5}(\text{PhCl})_{0.5}$. It follows from the analysis of the linewidths of the ESR spectra that the character of electron motion is quasi-one-dimensional in both crystals with identical orientation of conducting layers and the crystals with differently oriented layers. As it follows from the polarized reflectance spectra, the crystals with identical orientation of conducting layers are quasi-one-dimensional conductors and, in the case of the crystals with differently oriented layers, the conductivity is close to isotropic in two directions of the conducting plane. The electrical conductivity of compound $(\text{TMBEDT-TTF})_5\text{Hg}(\text{SCN})_{4-x}\text{I}_x$ with differently oriented conducting layers has almost isotropic character in two directions of the conducting plane. The crystals with identical orientation of conducting layers are characterized with a higher (by one order of magnitude) conductivity. The cumulative results allow one to conclude that the properties of organic conductors with differently oriented conducting layers and the quasi-one-dimensional character of electron motion are determined by superposition of the properties of individual layers.

Experimental

Electron probe microanalysis (EPMA). The compositions of the crystals of radical cation salts were established by EPMA with application of a CamScan MV 2300 electron microscope equipped with an energy-dispersive X-ray spectrometer with a semiconducting Si(Li) detector using the INCA Energy 200 software program at a thousandfold magnification and electron-beam energy of 20 keV. The depth of beam penetration into the sample was 1–3 μ . The crystals of reference compound $(\text{ET})_4\text{Hg}_2\text{Br}_6(\text{PhCl})$ were prepared according to a known procedure.²⁹

Conductivities of single crystals were measured by the standard four-probe method at direct current (10 μ A) on an automated device upon reduction of the temperature from 293 K to 20, 100, and 5 K for **1**, **2**, and **3**, respectively. Gold contacts (diameter 10 μ m) were glued to the crystal using a graphite paste.

Optical properties of crystals were studied on a FT-IR Perkin—Elmer 1725X spectrometer equipped with an infrared microscope having an effective diameter of light ray of 100 μ m and a flowing helium cryostat (Oxford Instruments). Polarized reflectance spectra in the frequency range of 650–7000 cm^{-1} were studied at room temperature at 8 K (salt **1** and **3**) and 5 K (salt **2**) from different sites of one or more crystals. Optical conductivity spectra were calculated from reflectance spectra using the Kramers—Kronig transformation on the assumption that the reflection index on the low frequencies behaves like that for semiconducting compounds at 300 K and by the standard extrapolation at high frequencies.³⁰ The reflectance spectra at 8 K in the low-frequency region were represented by a constant.

ESR spectra were measured using a RADIOPAN SE/X-2547 spectrometer with the modulation frequency of 100 kHz and the microwave power of 100 mW, which was equipped with Radiopan TC-660 and RR-221 cooling systems. The temperature was changed in the range of 300–90 K. The temperature dependences of the ESR linewidth (ΔH_{pp}) and spin susceptibility (χ) were measured at the vertical crystal orientation in a resonator (the long axis and planar surface of a crystal are arranged perpendicularly to the static magnetic field H_0). At such crystal orientation, the power absorption in the skin layer have no effect on the pattern of ESR spectrum.

Ethylenedithiotetrathiafulvalene (EDT-TTF) was synthesized by a known procedure.³¹ Bis(dimethylethylenedithio)-tetrathiafulvalene (TMBEDT-TTF) was prepared by the previously described procedure.²⁰

The salt $(\text{EDT-TTF})_3\text{Hg}_2\text{Br}_6$ (1**)** was prepared by electrochemical oxidation of EDT-TTF (8.8 mg, 0.03 mmol) in freshly distilled THF (11 mL) in the galvanostatic regime ($I = 0.5 \mu\text{A}$) at 18 °C. A mixture of $\text{Bu}_4\text{NHgBr}_3$ (6.8 mg, 0.01 mmol) and HgBr_2 (18 mg, 0.05 mmol) was used as a supporting electrolyte. The crystals of two phases, viz., the orthorhombic plates and thickened needles, formed simultaneously on a platinum anode for 15–18 days. According to the EPMA data, the S : Hg : Br atomic ratio is 9 : 1 : 3 for the plates, which corresponds to the formula $(\text{EDT-TTF})_3\text{Hg}_2\text{Br}_6$, and 6 : 1 : 3 for needles, which corresponds to the stoichiometric formula $(\text{EDT-TTF})_2\text{HgBr}_3$.

The salt $(\text{TMBEDT-TTF})_5\text{Hg}(\text{SCN})_{4-x}\text{I}_x$ ($x \approx 0.35$) (2**)** was prepared by electrochemical oxidation of TMBEDT-TTF (13.2 mg, 0.03 mmol) in a 10% solution of EtOH in PhCl (11 mL) in the galvanostatic mode ($I = 0.2 \mu\text{A}$) at –15 °C. A mixture of $[\text{Bu}_4\text{N}]\text{CsHg}(\text{SCN})_{3.5}\text{I}_{0.5}$ (34 mg, 0.04 mmol) and dibenzo-18-crown-6 (14.4 mg, 0.04 mmol) was used as a supporting electrolyte. The crystals in the form of elongated hexagonal plates was prepared for two weeks. According to the EPMA data, the S : Hg : I atomic ratio is 44 : 1 : (0.3–0.4), which corresponds to the formula $(\text{TMBEDT-TTF})_5\text{Hg}(\text{SCN})_{4-x}\text{I}_x$ ($x \approx 0.35$).

The salt $(\text{EDT-TTF})_3\text{Hg}(\text{SCN})_3\text{I}_{0.5}(\text{PhCl})_{0.5}$ (3**)** was prepared by electrochemical oxidation of EDT-TTF (8.8 mg, 0.03 mmol) in a 10% solution of EtOH in PhCl (9 mL) in the galvanostatic mode ($I = 0.35 \mu\text{A}$) at 15 °C. A mixture of $[\text{Bu}_4\text{N}]\text{CsHg}(\text{SCN})_{3.5}\text{I}_{0.5}$ (33 mg, 0.04 mmol) and dibenzo-18-crown-6 (14.4 mg, 0.04 mmol) was used as a supporting electrolyte. The crystals was obtained after two weeks. According to the EPMA data, the S : Hg : I : Cl atomic ratio is 20 : 1 : 0.5 : 0.5, which corresponds to the formula $(\text{EDT-TTF})_3\text{Hg}(\text{SCN})_3\text{I}_{0.5}(\text{PhCl})_{0.5}$.

This work was financially supported by the Presidium of the Russian Academy of Sciences (Program for Basic Research No. 27 "Fundamentals of Basic Research of Nanotechnologies and Nanomaterials"), the Division of Chemistry and Materials Science of the Russian Academy of Sciences, and the Russian Foundation for Basic Research (Project No. 08-03-00480a).

References

1. J. M. Williams, J. R. Ferraro, R. J. Thorn, K. D. Carlson, U. Geiser, H. H. Wang, A. M. Kini, M. H. Whangbo, *Or-*

- ganic Superconductors (Including Fullerenes): Synthesis, Structure, Properties and Theory*, Prentice Hall, Englewood Cliffs, New Jersey, 1992.
2. P. Batail, *Chem. Rev.*, 2004, **104**, 4887.
 3. R. B. Lyubovskii, R. N. Lyubovskaya, O. A. Dyachenko, *J. Phys. I*, 1996, **6**, 1609.
 4. J. A. Schlueter, U. Geiser, M. A. Whated, N. Drichko, B. Salameh, K. Petukhov, M. Dressel, *J. Chem. Soc., Dalton Trans.*, 2007, 2580.
 5. R. N. Lyubovskaya, E. I. Zhilyaeva, S. I. Pesotskii, R. B. Lyubovskii, L. O. Atovmyan, O. A. D'yachenko, T. G. Takhirov, *Pis'ma Zh. Eksp. Teor. Fiz.*, 1987, **46**, 149 [*JETP Lett. (Engl. Transl.)*, 1987, **46**, 188].
 6. E. I. Zhilyaeva, O. A. Bogdanova, R. N. Lyubovskaya, R. B. Lyubovskii, S. I. Pesotskii, J. A. A. J. Perenboom, S. V. Konovalikhin, G. V. Shilov, A. Kobayashi, H. Kobayashi, *Synth. Met.*, 2001, **120**, 1089.
 7. E. I. Zhilyaeva, A. Y. Kovalevsky, R. B. Lyubovskii, S. A. Torunova, G. A. Mousdis, G. C. Papavassiliou, R. N. Lyubovskaya, *Cryst. Growth Des.*, 2007, **7**, 2768.
 8. E. I. Zhilyaeva, R. N. Lyubovskaya, S. V. Konovalikhin, O. A. Dyachenko, R. B. Lyubovskii, *Synth. Met.*, 1998, **94**, 35.
 9. R. B. Lyubovskii, S. I. Pesotskii, S. V. Konovalikhin, G. V. Shilov, A. Kobayashi, H. Kobayashi, V. I. Nizhankovskii, J. A. A. J. Perenboom, O. A. Bogdanova, E. I. Zhilyaeva, R. N. Lyubovskaya, *Synth. Met.*, 2001, **123**, 149.
 10. E. I. Zhilyaeva, S. A. Torunova, R. N. Lyubovskaya, S. V. Konovalikhin, O. A. Dyachenko, G. V. Shilov, R. B. Lyubovskii, *Synth. Met.*, 1996, **79**, 189.
 11. E. I. Zhilyaeva, O. A. Bogdanova, V. V. Gritsenko, O. A. Dyachenko, R. B. Lyubovskii, K. V. Van, A. Kobayashi, H. Kobayashi, R. N. Lyubovskaya, *Synth. Met.*, 2003, **139**, 535.
 12. E. I. Zhilyaeva, S. A. Torunova, R. N. Lyubovskaya, S. V. Konovalikhin, G. V. Shilov, M. G. Kaplunov, E. V. Golubev, R. B. Lyubovskii, E. I. Yudanov, *Synth. Met.*, 1999, **107**, 123.
 13. M. Kurmoo, A. W. Graham, P. Day, C. J. Coles, M. B. Hursthouse, J. L. Caulfield, J. Singleton, F. L. Pratt, W. Hayes, L. Ducasse, P. Guionneau, *J. Am. Chem. Soc.*, 1995, **117**, 12209.
 14. O. N. Kazheva, N. D. Kushch, O. A. Dyachenko, E. Canadell, *J. Solid State Chem.*, 2002, **168**, 457.
 15. D. Vignolles, A. Audouard, R. B. Lyubovskii, S. I. Pesotskii, J. Beard, E. Canadell, G. V. Shilov, O. A. Bogdanova, E. I. Zhilyaeva, R. N. Lyubovskaya, *Solid State Sci.*, 2007, **9**, 1140.
 16. E. I. Zhilyaeva, O. A. Bogdanova, G. V. Shilov, R. B. Lyubovskii, S. I. Pesotskii, S. M. Aldoshin, A. Kobayashi, H. Kobayashi, R. N. Lyubovskaya, *Synth. Met.*, 2009, **159**, 1072.
 17. L. Martin, P. Day, H. Akutsu, J.-i. Yamada, S.-i. Nakatsuji, W. Clegg, R. W. Harrington, P. N. Horton, M. B. Hursthouse, P. McMillan, S. Firth, *Cryst. Eng. Commun.*, 2007, **9**, 865.
 18. J. A. Schlueter, U. Geiser, H. H. Wang, A. M. Kini, B. H. Ward, J. P. Parakka, R. G. Daugherty, M. E. Kelly, P. G. Nixon, G. L. Gard, L. K. Montgomery, H. J. Koo, M. H. Whangbo, *J. Solid State Chem.*, 2002, **168**, 524.
 19. T. Mori, N. Sakuray, S. Tanaka, H. Moriyama, *Bull. Chem. Soc. Jpn.*, 1999, **72**, 683.
 20. A. Karrer, J. D. Wallis, J. D. Dunitz, B. Hilti, C. W. Mayer, M. Burkle, J. Pfeiffer, *Helv. Chim. Acta*, 1987, **70**, 942.
 21. T. Mori, *Bull. Chem. Soc. Jpn.*, 1998, **71**, 2509.
 22. O. N. Kazheva, Ph.D. (Chem.) Thesis, Institute of Problems of Chemical Physics of the RAS, Chernogolovka, 2002, 155 pp. (in Russian)
 23. C. Coulon, R. Clerac, *Chem. Rev.*, 2004, **104**, 5655.
 24. R. B. Morgunov, A. A. Baskakov, L. R. Dunin-Barkovskii, L. V. Zorina, S. S. Khasanov, R. P. Shibaeva, T. G. Prokhorova, E. B. Yagubskii, T. Kato, I. Tanimoto, *Khim. Fiz.*, 2005, **24**, 88 [*Russ. J. Phys. Chem. B (Engl. Transl.)*, 2005, **24**].
 25. M. G. Kaplunov, Yu. G. Borod'ko, *Khim. Fiz.*, 1987, **6**, 1529 [*Sov. Phys. Chem. (Engl. Transl.)*, 1987, **6**].
 26. R. M. Vlasova, O. O. Drozdova, V. N. Semkin, N. D. Kushch, E. I. Zhilyaeva, R. N. Lyubovskaya, E. B. Yagubskii, *Fiz. Tverd. Tela*, 1999, **41**, 897 [*Phys. Sol. State (Engl. Transl.)*, 1999, **41**, 814].
 27. M. Dressel, N. Drichko, *Chem. Rev.*, 2004, **104**, 5689.
 28. M. J. Rice, *Phys. Rev. Lett.*, 1976, **37**, 36.
 29. R. N. Lyubovskaya, T. V. Afanas'eva, O. A. D'yachenko, V. V. Gritsenko, Sh. G. Mkoyan, G. V. Shilov, R. B. Lyubovskii, V. N. Laukhin, M. K. Makova, A. G. Khomenko, A. V. Zvarykina, *Izv. Akad. Nauk SSSR, Ser. Khim.*, 1990, 2872 [*Bull. Acad. Sci. USSR, Div. Chem. Sci. (Engl. Transl.)*, 1990, **39**, 2608].
 30. F. Wooten, *Optical Properties of Solids*, Academic Press, New York, 1972, 260 pp.
 31. R. Kato, H. Kobayashi, A. Kobayashi, *Chem. Lett.*, 1989, 781.

Received December 29, 2009;
in revised form March 10, 2010